Biogeosciences Discuss., 10, 18479–18514, 2013
www.biogeosciences-discuss.net/10/18479/2013/
doi:10.5194/bgd-10-18479-2013

Biogeosciences Discussions
Open Access

An inverse modeling approach for tree-ring-based climate reconstructions under changing atmospheric CO_2 concentrations

É. Boucher[1], J. Guiot[2], C. Hatté[3], V. Daux[3], P.-A. Danis[4], and P. Dussouillez[2]

[1]Dept of Geography and GEOTOP, Université du Québec à Montréal, Montréal, Canada
[2]CEREGE, Aix-Marseille Université CNRS UMR 7330, Europôle de l'Arbois, 13545 Aix-en-Provence, France
[3]LSCE-IPSL, UMR CEA-CNRS-UVSQ 8212, 12, L'Orme des Merisiers, 91191 Gif-sur-Yvette, France
[4]Onema-Irstea Hydro-écologie Plans d'Eau, 3275 Route de Cézanne, CS 40061, 13182 Aix-en-Provence, France

Received: 24 October 2013 – Accepted: 18 November 2013 – Published: 28 November 2013

Correspondence to: É. Boucher (boucher.etienne@uqam.ca)

Published by Copernicus Publications on behalf of the European Geosciences Union.

Abstract

Over the last decades, dendroclimatologists have relied upon linear transfer functions to reconstruct historical climate. Transfer functions need to be calibrated using recent data from periods where CO_2 concentrations reached unprecedented levels (near 400 ppm). Based on these transfer functions, dendroclimatologists must then reconstruct a different past, a past where CO_2 concentrations were much below 300 ppm. However, relying upon transfer functions calibrated in this way may introduce an unanticipated bias in the reconstruction of past climate, particularly if CO_2 levels have had a noticeable fertilizing effect since the beginning of the industrial era. As an alternative to the transfer function approach, we run the MAIDENiso ecophysiological model in an inverse mode to link together climatic variables, atmospheric CO_2 concentrations and tree growth parameters. Our approach endeavors to find the optimal combination of meteorological conditions that best simulate observed tree ring patterns. We test our approach in the Fontainebleau forest (France). By comparing two different CO_2 scenarios, we present evidence that increasing CO_2 concentrations have had a slight, yet significant, effect on reconstruction results. We demonstrate that higher CO_2 concentrations augment the efficiency of water use by trees, therefore favoring the reconstruction of a warmer and drier climate. Under elevated CO_2 concentrations, trees close their stomata and need less water to produce the same amount of wood. Inverse process-based modeling represents a powerful alternative to the transfer function technique, especially for the study of divergent tree-ring-to-climate relationships. The approach has several advantages, most notably its ability to distinguish between climatic effects and CO_2 imprints on tree growth. Therefore our method produces reconstructions that are less biased by anthropogenic greenhouse gas emissions and that are based on sound ecophysiological knowledge.

BGD
10, 18479–18514, 2013

1 Introduction

With climatic change and rising CO_2 concentrations, the need to place recent trends in a multi-secular perspective has led to an unprecedented expansion of the field of paleoclimatology. Tree rings have played a central role in that development, offering the possibility to reconstruct various climatic fields at high temporal resolution (annual to infra-annual) (e.g., Fritts, 1976; Schweingruber, 1996) and over large areas (regional, e.g., Cook et al., 2004, hemispheric, e.g., Esper et al., 2002; Briffa et al., 1998a; Mann et al., 1999 or global, e.g., Mann et al., 2008). To perform such reconstructions, dendrochronologists have typically relied upon various black-box approaches (also called transfer functions) (Fritts, 1976) that approximate relationships between tree rings and climate by a time-invariant function. However, evidence for nonstationarity and divergence in the biological response to climate have called into question the transfer function approach (Vaganov et al., 2006). Time-varying tree-ring-to-climate responses may have various origins (D'Arrigo et al., 2008): thresholded, complex and nonlinear responses, alteration of climate/growth relationships by CO_2 and sustained changes in water-table levels. If these phenomena are not accounted for in the reconstruction model, discrepancies between real and reconstructed paleoclimatic variability can be expected (Briffa et al., 1998b).

Since carbon dioxide is well mixed and homogeneously distributed throughout Earth's atmosphere (Myhre et al., 1998), CO_2 fertilization might be one of the most widespread source of divergence, but yet, its biological impact on climate-to-tree-growth relationships remains imprecise (D'Arrigo et al., 2008). However, since the beginning of the industrial period, CO_2 concentrations have increased by about 150 ppm, reaching 400 p.m. in 2013 (Tans and Keeling, 2013). If tree ring chronologies have been imprinted by a strong CO_2 signal during the late industrial period (LaMarche et al., 1984), it becomes quite risky to use transfer models calibrated against the recent decades to document paleoclimatic variations of pre-industrial periods where CO_2 concentrations were much lower (below 250 ppm).

Several alternatives to the transfer function approach exist, most of which make use of extensive process-based modeling. Data-assimilation approaches such as the one proposed by Goosse et al. (2010) aim at constraining climate models in order to identify plausible and coherent climatic scenarios that match the variations of natural proxies. Data-assimilation techniques allow to test various forcing scenarios, but in the case of tree rings, the linkages between climate simulations and proxies remain imprecise as signal and noise components cannot be clearly distinguished. In other fields of paleoclimatology, several authors have put forward the idea that deterministic models can be reversed so that the set of rules and mathematical equations representing the many processes that occur in ecosystems can be used in an inverse mode to retrieve probabilistic estimates for input meteorological conditions (Chuine et al., 2004; Hughes and Ammann, 2009; Guiot et al., 2000, 2009; de Cortázar-Atauri et al., 2010; Evans et al., 2013). This approach has been tested by Garreta et al. (2010) for pollen data, but yet, no dendroecological model was inverted to perform a reconstruction. Tolwinski-Ward et al. (2011) have recently accomplished a first step towards the reconstruction and used a simplified version of the Vaganov–Shashkin model (VS-lite) that mimics the principle of limiting factor to simulate thresholded ring width responses. However, while they claim that a simple water bucket model is more efficient computationally in the perspective of an inversion, some of the most important ecophysiological processes responsible for tree growth in nature (e.g. to name a few: the influence of CO_2 on photosynthesis, resource allocation and partitioning of carbon, reuse of preceding year's photosynthetates, etc) are omitted, with uncertain consequences for the inversion. Plus, the focus is on a single proxy (ring widths) while it has been demonstrated that a multi-proxy approach is the most efficient way to enhance long-term environmental signals (McCarroll and Loader, 2004; Mann, 2002). Variables such as oxygen and carbon isotopes in tree-ring cellulose are now routinely measured, so inverse modeling approaches should account for these proxies that present complementary (different) signals (sources of noise).

Here we present a reconstruction performed from the inversion of the MAIDENiso model (Danis et al., 2012), an updated version of the MAIDEN model (Misson, 2004) that accounts for carbon and oxygen isotope fractionation. MAIDENiso is a full ecophysiological model, meaning that the links between meteorological (input) variables and (output) tree ring variables (e.g tree ring widths, carbon and oxygen isotopes) are not empirically parametrized as in a regression, but explicitly represented as mathematical equations within the model. The main objective of this paper is to demonstrate the scientific and conceptual advantages that invert dendroclimatological modeling may have for the study of past climates. With this objective in mind, we will address the following questions: (1) How good are the reconstructions performed from the inversion? (2) Are they better than traditional transfer function techniques based, for example, on linear modeling? (3) Is the approach able to take into account and eventually isolate the effect of CO_2 fertilization on tree ring growth and thus, attests of its impact on past climates reconstructed from tree ring series?

This paper will be divided in two parts. In the first part, we rapidly review the model's capability as well as its parametrization. We then present our inversion approach explicitely. In the second part, we apply the inversion technique to reconstruct past climatic variations in the Fontainebleau Forest (near Paris, France), where Danis et al. (2012) have recently calibrated the model.

2 MAIDENiso

MAIDENiso is a process-based, dendrogeochemical model that can simulate various tree growth parameters useful in dendroecological analysis such as tree ring widths, $\delta^{18}O$ and $\delta^{13}C$ of tree ring cellulose. Earlier versions of the model were used to simulate tree growth in northern and southern France (Gaucherel et al., 2008; Misson et al., 2004), as well as Belgium (Misson, 2004). Recently, the model was completed by Danis et al. (2012) to capture the main variations of $\delta^{18}O$ and $\delta^{13}C$ of tree ring cellulose found in sessile oak (*Quercus petraea* Matt.). In the forward mode, it uses relatively simple

BGD
10, 18479–18514, 2013

meteorological inputs: daily precipitation ($cm\,d^{-1}$), minimum and maximum temperature (°C). However, other variables are also required (on a daily basis) such as atmospheric concentration of CO_2 (ppm), the content of $\delta^{18}O$ of precipitation, and $\delta^{13}C$ content in atmospheric CO_2. Lastly, a limited amount of parameters need to be found in the literature or estimated directly from tree rings using optimization techniques (see Gaucherel et al. (2008) and Misson et al. (2004), for more explanations).

MAIDENiso captures and models site-specific phenological as well as meteorological controls on transpiration, stomatal conductance, respiration and photosynthetic production. For an extensive review of the processes and how they are modeled, readers are referred to the original works by Misson (2004) and Danis et al. (2012). The algorithm includes several allocation rules that distribute biomass production, carbon and oxygen isotopes in various reservoirs such as leafs, bole, roots, and storage. From a dendroecological perspective, bole is the most important reservoir, as it can be readily compared to standard tree ring measurements such as tree ring widths, $\delta^{18}O$ and $\delta^{13}C$. However, storage is an another important property of the model as it allows to simulate processes responsible for autocorrelation and persistence in tree growth parameters, therefore enabling the use of carbohydrates to be passed to the next year of simulation. This aspect has important implications in ecology but also in paleoclimatology. For example, in the case of the Fontainebleau forest (described later) (Danis et al., 2012) argued that an adequate modeling of storage reserves by MAIDENiso allowed for a proper simulation of the 1976 drought in that area. In the years following the drought, and in spite of the amelioration of climatic conditions, trees were unable to store a sufficient amount of reserves which resulted in sustained growth reductions. From a paleoclimatological perspective, it is important that the inversion distinguishes between climatic and storage-related effects. Otherwise, prolonged ecophysiological responses could be mistaken for persistent harsh climatic conditions.

BGD
10, 18479–18514, 2013

3 MAIDENiso's inversion procedure

The inversion approach described here (Fig. 1) allows to retrieve paleoclimatic information from ecophysiological models. The method is presented with examples from the Fontainebleau forest (France). First, it must be stated that inverse modeling procedures do not aim at finding a backward solution to the set of rules and equations that are implemented in a process-based model. Instead, inverse modeling approaches seek at finding the optimal combination of input data so that outputs (i.e. simulations) are as close as possible to the observations. In the precise context of dendroecological modeling, inverting a model such as MAIDENiso implies finding the optimal combination of meteorological inputs that will best simulate tree ring parameters (tree ring widths, $\delta^{18}O$ and $\delta^{13}C$). Consequently, the model has to be run repeatedly with different meteorological scenarios each time, preserving only the ones that simulate tree ring parameters that resemble observations, and eliminating the rest.

So, at first glance, a contradiction seems to emerge: the model has to be run with meteorological data to produce tree ring simulations, but, in the case of a climate reconstruction, it is precisely those conditions that are unknown. Therefore, the general strategy proposed here is to define, from the modern dataset, a reference or average meteorological year (AMY) that will serve as a basis to produce alternative meteorological scenarios (Fig. 1). Identifying the AMY ensures that a certain degree of temporal coherence exists in the relationship between temperatures and precipitation. In the case of the Fontainebleau forest, the meteorological dataset originaly used by Danis et al. (2012) corresponds to the average of two stations (Glandée at Villiers-en-Bière and Faissandière at Fontainebleau) located 10 km north of the forest. From this dataset and with a simple measure of euclidian distance, we identified year 1984 as the one that is closest, in terms of average temperature and precipitation (spring and summer) to the 1953–2000 average (Fig. 2a and b). Figure 2c and d presents temperature and precipitation variations that occurred in 1984, at Fontainebleau. The temperature curve presents a typical hyperbolic shape with an average temperature of 10.2 °C. The precipitation series depicts considerable variability at the daily to monthly scales, with low summer precipitation and precipitation peaks in june (4.5 cm) and september (3.8 cm) respectively, and with an average of 0.27 cm precipitation per day.

Once the AMY is identified, the next step is to find a way to modify it in order to produce alternative meteorological scenarios (AMS) that will be iteratively re-injected within MAIDENiso, through the undermentioned inversion algorithm. The strategy proposed here is to modify the AMY's original temperature and precipitation series with constants (thereafter named deltas, or Δ), that generate AMS. For each year simulated, we defined two different Δ, one for temperature (Δ_τ) that is additive and a second for precipitation (Δ_π) that is multiplicative. They both apply during the growing season, which is defined here as the period between early April (julian day 91) and late October (julian day 304). Figure 2c and d presents two alternative meteorological scenarios computed from two different Δ_τ and Δ_π values. In the first scenario (red), Δ_τ and Δ_π were assigned a value of 2, meaning that all days are incremented positively by 2 °C, and that all precipitation events, when they occur, are doubled in magnitude. In the second scenario (blue), we assigned values of −2 and 0.5 to Δ_τ and Δ_π, respectively. Therefore, two degrees were subtracted to the temperature series and the daily amount of precipitation was halved during the growing season.

Δ_τ and Δ_π were implemented so that the modifications of meteorological conditions by the Metropolis–Hasting's algorithm (described hereafter) are kept as simple and straigthforward as possible. But the modifications themselves must be confined within bounds that respect the properties of local climatology in order to avoid generating implausible meteorological conditions. Uniform priors are then set to Δ_τ and Δ_π, with values bounded between −5 and +5 for the former and between 0.25 and 4 for the latter. Such values produce bounds that are larger than the modern (1950–2000) interannual meteorological variability, but were set uniform because we assumed to have no a priori knowledge on past fluctuations within these bounds. Moreover, Gaussian priors centered around AMY would give too much weight to the “normal” conditions and are likely to be incompatible with our wish to generate sufficiently different climatic conditions from the present ones.

The Metropolis Hastings random walk algorithm (MHA) is used to estimate, for each year t of the reconstruction the posterior probability distribution of $\Delta_{\tau(t)}$ and $\Delta_{\pi(t)}$. The MHA is a Markov Chain Monte Carlo (MCMC) procedure and therefore sample candidates produced within the chain depend only on the current sample value. The chain progresses towards a stable state by accepting or rejecting proposed samples. Concerning our application, the posterior distribution of $\Delta_{\tau(t)}$ and $\Delta_{\pi(t)}$ corresponds to the distribution of accepted values that best simulate tree ring parameters, at year t.

The MHA is extensively described in Hastings (1970); here, the most important principles will be presented and exemplified with our tree ring application (Fig. 1). For each meteorological year t to be reconstructed from tree ring parameters, let $f(\Delta_t)$ be a target density that is proportional to the desired probability distribution of Δ at year t, $P(\Delta_t)$. First, $f(\Delta_t)$ executes a MAIDENiso run through which tree ring parameters are simulated given input AMS. Then a metric λ (Fig. 1) needs to be maximized $[-\infty \rightarrow 0]$ and corresponds to the negative squared distance between simulated (s) and real world observations (o):

$$\lambda_t = -(\delta^{13}\mathrm{C}_{t(s)} - \delta^{13}\mathrm{C}_{t(o)})^2 - (\delta^{18}\mathrm{O}_{t(s)} - \delta^{18}\mathrm{O}_{t(o)})^2 - (\mathrm{TRW}_{t(s)} - \mathrm{TRW}_{t(o)})^2 \qquad (1)$$

To calculate λ, all tree ring variables are transformed into dimensionless standardized scores. From there, the MHA starts by defining current values for $\Delta_{\tau t(i)}$ and $\Delta_{\pi t(i)}$ (hereafter grouped into $\Delta_{t(i)}$) that fall within the bounds of a uniform prior distribution $q(\Delta_t|\Delta_{t(i)})$. The algorithm then defines a candidate set of deltas: Δ_t^*. The chain M walks towards the next iteration, accepting or rejecting the candidate values according to the following rules:

$$M = \begin{cases} P\left(\Delta_{t(i)}, \Delta_t^*\right) & \text{if } f(\Delta_t^*) \geq f\left(\Delta_{t(i)}; (\text{accept } \Delta_t^*)\right) \\ P\left(\Delta_{t(i)}, \Delta_t^*\right)\alpha & \text{if } f\left(\Delta_t^*\right) < f\left(\Delta_{t(i)}; \left(\text{accept } \Delta_t^* \text{ with } \alpha = e^{f(\Delta_t^*) - f(\Delta_{t(i)})}\right)\right) \\ P\left(\Delta_{t(i)}, \Delta_{t(i+1)}\right)(1-\alpha) & \text{if } \alpha < 1; (\text{reject} \Delta_t^* \text{ with } 1-\alpha) \end{cases} \qquad (2)$$

In other words, if $f(\Delta_t^*) \geq f(\Delta_{t(i)})$, then the candidate set Δ_t^* is more likely than the original set of deltas to produce tree ring parameters that mimic those found in nature. In that case, Δ_t^* is accepted with probability = 1 and the algorithm "walks" to the next iteration replacing $\Delta_{t(i+1)}$ by Δ_t^*. In the case where $f(\Delta_t^*) < f(\Delta_{t(i)})$, there are two possibilities. First, there is a chance equal to α that Δ_t^* is accepted and passed to the next iteration. Second, there is a $1-\alpha$ chance that Δ_t^* is rejected and consequently, $\Delta_{t(i)}$ is maintained at the next iteration. After a large number of iterations, the chain M will tend to be proportional to $P(\Delta_t)$ because the algorithm will be "intuitively" visiting high density regions more often than it does for low density regions.

The inversion scheme presented earlier (Fig. 1) enables to sample in the posterior distribution $P(\Delta_t)$ one year at a time. However, tree rings series usually present a certain degree of autocorrelation. Such a persistence may be caused by climatic variations, but may also result from persisting insufficient carbon storage. Fortunately, MAIDENiso can account for storage and remobilization of carbon reserves within the tree, but to do so, it needs to simulate more than a single year at a time. In order to correctly model autocorrelation, we opted for a four-year block simulation (Fig. 3). Thus, to obtain a distribution for Δ_t, we fed MAIDENiso with Δ_{t-1}, Δ_{t-2}, Δ_{t-3} that are passed from the preceding simulations (dashed lines on Fig. 3). Hence, all four Δ respectively modify the AMY (year 1984) to produce four-year-long daily temperature and precipitation series that are used by MAIDENiso. Accordingly, simulated tree ring series exhibit a four-year dependance structure that should be similar to the one observed in real world samples. Median $\Delta_{\tau(t)}$ and $\Delta_{\pi(t)}$ values are passed to the subsequent year and so forth (Fig. 3). It is important to underline that the optimization of the metric λ (Eq. 1) by the MHA is exclusively performed for the last year of the simulation, irrespective of the number of years included in the simulation.

4 Application of the inversion algorithm to the Fontainebleau forest (France)

4.1 Tree ring data

All tree ring data (Fig. 4) used for the inversion are latewood measurements previously published by Etien et al. (2008). Thirty living, dominant oaks were sampled in the Fontainebleau forest (two stations, $N = 15$/station). On each tree, three cores were sampled at 1.3 m of height. Each series was measured and cross-dated by the phytoecology team of the National Institute of Agronomical Research (INRA, Nancy, France) using a master chronology constructed from more than 400 oaks sampled in the nearby area. The living tree chronology was standardized using the adaptive regional growth curve technique (Nicault et al., 2010) to produce an average chronology (Fig. 4a). Each tree rings were then cut using a scalpel to separate latewood from earlywood. Samples were pooled and then milled with a 80 micron sieve. α-cellulose was extracted using the SOXHLET method (Leavitt and Danzer, 1993). Isotopic compositions (Fig. 4b and c) were determined with a Carbo Erba elemental analyser coupled to a Finnigan MAT252 mass spectrometer (at LSCE, Gif/Yvette, Fr). Correction of cellulose $\delta^{13}C$ series for the Suess effect was not necessary since in MAIDENiso, atmospheric $\delta^{13}C$ is used as an input and the model directly yields depleted series comparable to those found in tree rings.

4.2 Atmospheric data

In addition to tree ring and meteorological data, three additional variables were prescribed as inputs to MAIDENiso: atmospheric CO_2 concentrations, atmospheric $\delta^{13}C$ content and $\delta^{18}O$ of precipitation. CO_2 concentrations and atmospheric $\delta^{13}C$ were both derived from published ice core data and were scaled with observations at the nearest CO_2 records (Gif-sur-Yvette, France) while $\delta^{18}O$ of precipitation ($\delta^{18}O_p$) was estimated statistically:

BGD
10, 18479–18514, 2013
Invert modeling of tree rings
É. Boucher et al.

- Atmospheric CO_2 concentrations. We retained two scenarios that will help us identify plausible fertilization effects and corresponding bias within the reconstruction (Fig. 5). The first scenario ("A1") mimics the reality and depicts a progressive increase in CO_2 concentrations towards modern values. The nearest CO_2 record (Gif-sur-Yvette) covers the 2000–2007 period. Only the mean annual cycle was retained from that short series and was superimposed over the long-term trend in CO_2 concentrations extracted from ice cores Robertson et al. (2001). The latter reflects global rather than local trends in CO_2. Therefore, both series were combined into a single one and simply extrapolated at the daily time step as in Danis et al. (2012). Scenario "A1" was also shifted by +15 ppm by comparison to the ice core series to take into account observable differences between the two series during their common period. The second scenario ("A2") represents a fictive situation into which CO_2 concentrations have remained stable (at pre-industrial levels) over the full reconstruction period. Scenario "A2" simply consists in the replication of year 1850 of scenario "A1" 151 times (1850–2000).

- Atmospheric $\delta^{13}C$ content. Atmospheric $\delta^{13}C$ data (Fig. 5) was retrieved from published ice core series (Francey et al., 1999) and covers the full reconstruction period. Modern annual cycles were extracted from the Schauinsland dataset (Black Forest, Germany) (Schmidt et al., 2003; Danis et al., 2012) that extends back to ca 1976. As for CO_2 trends, the Schauinsland annual cycle was superimposed over the long-term trend extracted from the ice core series. The resulting series was shifted by 1 ‰ towards lighter ratios to match values observed during the common period at Schauinsland.

- $\delta^{18}O$ of precipitation. We used the $\delta^{18}O_p$ data modeled by Danis et al. (2012). $\delta^{18}O_p$ was modeled statistically using linear regressions with temperature and precipitation. Daily $\delta^{18}O_p$ (dependent variable) as well a meteorological drivers (regressors) were extracted from the meso-scale climate model REMOiso (Sturm et al., 2005). The parameters were directly incorporated to MAIDENiso's code so

Discussion Paper | Discussion Paper | Discussion Paper | Discussion Paper |

BGD

10, 18479–18514, 2013

Invert modeling of tree rings

É. Boucher et al.

that the modeling of $\delta^{18}O_p$ could be achieved at each time step. Such parameters are site-specific.

4.3 Method of inversion–run details

In this study, Metropolis Hasting analysis were performed using the R statistical software (R Core Team, 2012), most particularly through the `metrop()` function of the `mcmc` package (Geyer and Johnson, 2012). For each year t simulated by the MHA, 500 burn-in samples were generated. Also, to ensure that the chain M is stable and composed only of successively uncorrelated and independent candidates, we picked only one Δ_t candidate at each 100 accepted samples. In total, we sampled 1000 candidate values for Δ_t. We finally verified that the chain convergence by checking that the lag-1 correlation between successive candidate values remained below 0.35.

5 Results and discussion

Here we present a paleoclimatic reconstruction for the Fontainebleau forest area, based on the inversion of the MAIDENiso model. The reconstruction extends back to ca 1850 and focuses on summer (JJA) temperature and precipitation. The A1 CO_2 scenario is used, unless the contrary is mentioned.

5.1 Comparison with modern climatic records

A comparison between reconstructed and observed summer climatic conditions is presented on Fig. 6 for the 1960–1999 period. The visual correspondence between both variables is fairly good, but slightly better for precipitation, both in terms of high frequency and low frequency variability. Reconstructed temperatures correlate well ($r = 0.53$) with observations (Table 1, column 1), but precipitation correlates even better ($r = 0.67$). As it is the case for observed chronologies (Table 1, column 2) temperature signal is weaker then precipitation signal. In other words, the climatic signal recorded

BGD
10, 18479–18514, 2013

by trees seems to be well extracted by our reconstruction. Moreover, as the model was already parametrized by Misson (2004) for tree rings and by Danis et al. (2012) for C and O isotopic fractionation, we argue that this climate reconstruction is coherent with the main ecophysiological processes that govern tree growth at Fontainebleau.

In the present simulation, a single $\Delta_{\tau(t)}$ and $\Delta_{\tau(t)}$ value now modifies the AMY to generate AMS, but ultimately, the comparison is made only for the summer period, owing to the fact that all proxies were measured on latewood. Consequently, all AMY are modified identically between day 91 and day 304, with no distinction between spring and summer conditions. Accordingly, by increasing the number of parameters to be estimated one would certainly augment the resolution of the ecophysiological modeling, therefore allowing seasonal reconstructions to be performed. Paleotemperature modeling would certainly benefit from such an approach because, even more important for tree growth than absolute temperatures is the length of the growing season. For instance no parameters modify the length of the growing season which is fixed to exactly 214 days. Further modeling efforts will be invested in order to increase the number of parameters to take into account varying growing season length as well as seasonal differences between spring and summer. However, it remains to be demonstrated that the Metropolis Hastings algorithm can still converge when the number of parameters is increased.

5.2 Reconstruction back to ca 1850

We extended the reconstruction back to AD 1850 and compared it to the Climate Research Unit (CRU) gridded temperature and precipitation reconstructions (Fig. 7). The general agreement between both series is fairly good, with, again, a clear visual correspondence in the high and low frequency domains. The correlations with the CRU data are 0.51 and 0.40 respectively for temperature and precipitation ($n = 100$ for precipitation and $n = 150$ for temperature). The temperature reconstruction seems to be in phase with the CRU data and the correlation is similar to that calculated on the 1960–1999 period. (Fisher r to z score $= -0.15$, $p > 0.05$). There is, however, a clear drop in the strength of the correlation for the precipitation (Fisher r to z score = 2, $p < 0.05$). While this drop could be interpreted as a flaw of the method, some other aspects must be considered. First, CRU data correlates poorly with precipitation at Fontainebleau over the 1960–1999 period ($r = 0.37$), so there is no reason to assume that both series did correlate well in the past. Second, it is clear from the visual examination of both curves that low frequencies are well reconstructed. Such low-frequencies may relate to the regional trend. However, high frequency variations of precipitation are difficult to interpolate at the local scale, especially in the Paris area where a temperate-oceanic climate dominates, with an important influence of convective precipitation during the summer. This kind of precipitation may be hard to interpolate and therefore, divergence can be expected with observations.

Inversions were compared to the reconstructions obtained from calibrating transfer functions (multiple linear regression) on the 1960–1999 period (Fig. 8). Although both techniques produce temperature and precipitation reconstructions that correlate well with one another, ($r = 0.74$ and 0.84, respectively), several differences need to be underlined. At first, a simple comparison of the variance for the pre-1950 and post-1950 period shows that the transfer function leads to an underestimation of the variance of temperatures for the last 50 yr. Taking the CRU (temperature) variance as a reference for the pre-1950 period (0.9), the variance obtained by inversion is 0.91 and the transfer function produces a comparable series (variance = 0.89). However, for the 1950–2000 period, the CRU variance augments to 1.16. The inversion follows that trend (post-1950 variance = 1.12) while the transfer function does not and the variance remains low (0.81) after 1950. This is a very important point, as variance loss and underestimation have plagued the transfer function approach over the last decade (Bürger, 2007) and may suggest that model inversions have a slight advantage over transfer functions from this point of view. For precipitation, all three method produce series with comparable variances for both pre-1950 (0.90 ± 0.1) and 1950–2000 periods. Nevertheless, the transfer function methods creates a slight but significant ($p < 0.01$, $n = 150$) positive trend in the amount of summer precipitation. Such a trend leads to an underestimation

Discussion Paper | Discussion Paper | Discussion Paper | Discussion Paper |

BGD

10, 18479–18514, 2013

Invert modeling of tree rings

É. Boucher et al.

of summer precipitation before 1900 and to a slight overestimation from 1950 onward. Such a trend does not exist neither in the inversion nor in the CRU precipitation series over the last century ($p > 0.05$).

In addition to reproduce variance and trends that characteristise Fontainebleau's climate, the inversion approach seems to have other conceptual advantages. By contrast to traditional transfer functions, no calibration is required, except for the initial parametrization of the ecophysiological model (here, MAIDENiso). Consequently, we expect our method to be more adaptable to the modeling of nonstationary tree-ring-to-climate relationships. Our inversion procedures also builds on sound ecophysiological knowledge and therefore the links between climate and tree growth are not reduced to a set of calibrated parameters, but are modeled with regards to the complexity and multiplicity of processes that control vegetation growth. From a modeling perspective, it is clear that each and every improvement made within the plant ecophysiology science community will directly translate to better reconstruction performances, and a greater adaptability of the model to a wide range of environments.

5.3 Impact of CO_2 on the reconstruction

MAIDENiso is an ecophysiological model that simulates tree growth parameters, given atmospheric inputs such as concentrations in CO_2 and $\delta^{13}C$. Therefore, the model can be used as a testbed to evaluate the impact, among other things, of CO_2 increases on the reconstruction. As mentioned earlier, we performed two reconstructions, each with a different CO_2 scenario (Fig. 4): scenario A1 which corresponds to the typical anthropogenically-modified curve and A2 which represents the non-anthropogenic curve (CO_2 remains stable).

A1 and A2 simulations yield quite different temperature and precipitation reconstructions (Fig. 8). Both reconstructions correlate well with one another ($r = 0.75$ for temperature, and $r = 0.87$ for precipitation), implying that high frequency variations are well reconstructed using both scenarios. However, temperature and precipitation series exhibit different long-term trends. Temperatures reconstructed using the A1 scenario shows a clear rise towards warmer conditions, while temperatures reconstructed using the A2 scenario remained stable over time. Contrastingly, from the point view of precipitation, the A1 scenario produces a drier climate then the A2 scenario. These results might point out at a fertilization effect by CO_2.

In order to better understand the effect of CO_2 on paleoclimate reconstructions, we re-injected both A1 and A2 reconstructions within the MAIDENiso model and run it in the forward mode. This allowed us to do two things. First, proxies as they were simulated in each run could be retrieved and compared to observed tree ring series. Without surprise, no matter which CO_2 scenario is chosen for the inversion, the MHA has systematically, but randomly, "walked" towards the best way to modify the Δ so that simulations match observations, with the constraint that λ should remain as close to zero as possible. We could verify that simulated values for each tree ring proxy and for each scenario are strongly related to original observations (Fig. 4, dashed lines). Second, running MAIDENiso in the forward mode allowed us to retrieve directly from the model and for each scenario, the variables that are required to estimate water use efficiency (WUE) of plants (Farquhar and Richards, 1984) such that:

$$\mathrm{WUE}_t = A/g = C_\mathrm{a}[1 - C_\mathrm{i}/C_\mathrm{a}]/1.6 \qquad (3)$$

where C_i and C_a correspond to the ratio between internal and atmospheric CO_2 concentrations, respectively. WUE ($\mu\mathrm{mol\,mol}^{-1}$) is a common way to express the ratio between photosynthetic biomass production (A) and stomatal conduction (g) and describes the tradeoff between carbon gain and water loss (Farquhar and Richards, 1984), i.e. the number of mole of carbon above ground divided by the number of moles of water transpired during the growth period.

WUE calculations were performed for both A1 and A2 CO_2 scenarios (Fig. 9). An increase in WUE efficiency is depicted for the A1 scenario while WUE remained stable over time when the reconstruction is forced by the A2 scenario. Thus, our results suggest that anthropogenic CO_2 concentrations at Fontainebleau led to a more efficient utilization of water resources by the plant, a result that is in accordance with recent studies conducted at the scale of the boreal and temperate forests of the Northern Hemisphere, over the last two decades (Keenan et al., 2013). Our study suggests that such processes acting at the hemispheric scale on WUE were also active at least over the last century in the Fontainebleau forest.

Increasing atmospheric CO_2 concentration is associated with enhanced biomass production in most parts of the world (LaMarche et al., 1984). Under elevated CO_2 concentrations, stomata do not need to remain wide open to maintain internal carbon concentrations (Keenan et al., 2013). Partial stomatal closure implies a greater water retention and an increased biomass production per unit of water absorbed by the plant. In the Fontainebleau context, higher WUE means that more carbohydrates are produced and stored per unit water absorbed, therefore forcing the inversion algorithm to converge towards higher temperatures to sustain growth rates. Complementarily, partial stomatal closure implies that less precipitation is required to sustain growth rates similar to those observed in nature, a result that ultimately generates a drier climate at Fontainebleau.

Our results finally imply that WUE of oak trees at the Fontainebleau forest augments with increasing concentrations of CO_2 in the atmosphere. The rate at which WUE augments with respect to CO_2 can be evaluated by plotting the difference in CO_2 concentrations and WUE for both A1 and A2 scenarios. The relationship between both variables is a straight line with a slope equal to 0.58. Thus, for each increment of 10 ppm of CO_2 in the atmosphere, WUE increases by 6 $\mu mol\,mol^{-1}$. This rate of increase in WUE might be downgraded by various acclimation processes to long term CO_2 increases (Drake et al., 1997): decrease in Rubisco, augmentation of carbohydrate solubility, increases in light use efficiency, lower rates of dark respiration. These processes are not well documented and are not (fully) integrated to the present version of MAIDENiso. Clearly, additional research is required to shed light on these processes so that they can be included and account for in the simulations in both forward and inverse mode. Recent works (Medlyn et al., 1999) have nevertheless suggested that such acclimation

BGD
10, 18479–18514, 2013

processes and the interactions between them never completely balance the net carbon gains related to a CO_2 enriched atmosphere.

While CO_2 concentrations in the atmosphere are continually increasing, it is clear that, as time passes, oaks at Fontainebleau will respond positively by augmenting WUE. As WUE increases, divergence in climate-to-tree-growth relationships such as the ones presented here are also expected to amplify, discouraging even more the use of transfer functions to perform paleoclimatic reconstructions. We argue that the approach presented here and based on the inversion of an ecophysiological model is best suited to perform paleoclimatic reconstructions under changing CO_2 concentrations and nonstationnary tree-ring-to-climate responses.

6 Conclusions

In this study, we demonstrated that the MAIDENiso ecophysiological model can be used to perform paleoclimatic reconstructions that take into account the effect of anthropogenic CO_2 concentrations on tree growth. We provided a way to inverse that model through the use of a random walk Metropolis Hastings that iteratively converges towards the best combination of meteorological conditions to fit observations. The approach was exemplified in a reconstruction of past summer temperatures and precipitation in the Fontainebleau forest (France). The novel reconstruction technique seems to perform well in that environment, and presents significant conceptual advantages comparing to the regression technique. Inversions are based on sound ecophysiological knowledge and on rules that can account for non-linear and complex interactions between tree rings, climate and CO_2. Hence, ecophysiological models such as MAIDENiso can be driven by different CO_2 scenarios to isolate any fertilization effects and divergent relationships between tree ring records and climate. Our work reveals that, at the Fontainebleau forest, CO_2 fertilization effect was significant and affected the trends of reconstructed climate towards warmer and drier summer conditions, mainly because trees growing in a CO_2 enriched atmosphere close their stomata and utilize water resources more efifciently. Although this analysis remains a first step towards a more generalised utilization of ecophysiological models in paleoclimatology, inversion approaches hold great promise in the context of continually rising CO_2 concentrations in the atmosphere. In years to come, the performance of the approach will likely increase, as a result of the amelioration of equations and rules within ecophysiological models, the improvement of random-walk algorithms, and the design of better parametrization strategies.

Acknowledgements. The first author sincerely thanks the Fonds de Recherche Nature et Technologies (FRQNT) for a post-doctoral scholarship. This work is a contribution to the Labex OT-Med (ANR-11-LABEX-0061) funded by the "Investissements d'Avenir", French Government program of the French National Research Agency (ANR) through the A*Midex project (ANR-11-IDEX-0001-02). Financial support was also provided by the ARCHIVES project funded by the Natural Sciences and Engineering Research Council of Canada (NSERC) as part of a collaborative research and development grant with OURANOS and Hydro-Québec.

References

Briffa, K., Jones, P., Schweingruber, F., and Osborn, T.: Influence of volcanic eruptions on Northern Hemisphere summer temperatures over the past 600 years, Nature, 393, 450–454, 1998a. 18481

Briffa, K., Schweingruber, F., Jones, P., Osborn, T., Harris, I., Shiyatov, S., Vaganov, E., and Grudd, H.: Trees tell of past climates: but are they speaking less clearly today?, Philos. T. Roy. Soc. B, 353, 65–73, 1998b. 18481

Bürger, G.: On the verification of climate reconstructions, Clim. Past, 3, 397–409, doi:10.5194/cp-3-397-2007, 2007. 18493

Chuine, I., Yiou, P., Viovy, N., Seguin, B., Daux, V., and Ladurie, E. L. R.: Historical phenology: grape ripening as a past climate indicator, Nature, 432, 289–290, 2004. 18482

Cook, E., Woodhouse, C., Eakin, C., Meko, D., and Stahle, D.: Long-term aridity changes in the western United States, Science, 306, 1015–1018, 2004. 18481

Danis, P.-A., Hatté, C., Misson, L., and Guiot, J.: MAIDENiso: a multiproxy biophysical model of tree-ring width and oxygen and carbon isotopes, Can. J. Forest Res., 42, 1697–1713, 2012. 18483, 18484, 18485, 18490, 18492

D'Arrigo, R., Wilson, R., Liepert, B., and Cherubini, P.: On the "divergence problem" in northern forests: a review of the tree-ring evidence and possible causes, Global Planet. Change, 60, 289–305, 2008. 18481

de Cortázar-Atauri, I. G., Daux, V., Garnier, E., Yiou, P., Viovy, N., Seguin, B., Boursiquot, J., Parker, A., Van Leeuwen, C., and Chuine, I.: Climate reconstructions from grape harvest dates: methodology and uncertainties, Holocene, 20, 599–608, 2010. 18482

Drake, B. G., Gonzàlez-Meler, M. A., and Long, S. P.: More efficient plants: a consequence of rising atmospheric CO_2?, Annu. Rev. Plant Biol., 48, 609–639, 1997. 18496

Esper, J., Cook, E., and Schweingruber, F.: Low-frequency signals in long tree-ring chronologies for reconstructing past temperature variability, Science, 295, 2250–2253, 2002. 18481

Etien, N., Daux, V., Masson-Delmotte, V., Stievenard, M., Bernard, V., Durost, S., Guillemin, M. T., Mestre, O., and Pierre, M.: A bi-proxy reconstruction of Fontainebleau (France) growing season temperature from A.D. 1596 to 2000, Clim. Past, 4, 91–106, doi:10.5194/cp-4-91-2008, 2008. 18489

Evans, M. N., Tolwinski-Ward, S., Thompson, D., and Anchukaitis, K. J.: Applications of proxy system modeling in high resolution paleoclimatology, Quaternary Sci. Rev., 76, 16–28, 2013. 18482

Farquhar, G. and Richards, R.: Isotopic composition of plant carbon correlates with water-use efficiency of wheat genotypes, Funct. Plant Biol., 11, 539–552, 1984. 18495

Francey, R., Allison, C., Etheridge, D., Trudinger, C., Enting, I., Leuenberger, M., Langenfelds, R., Michel, E., and Steele, L.: A 1000-year high precision record of $\delta^{13}C$ in atmospheric CO_2, Tellus B, 51, 170–193, 1999. 18490

Fritts, H.: Tree Rings and Climate, Elsevier, 1976. 18481

Garreta, V., Miller, P. A., Guiot, J., Hély, C., Brewer, S., Sykes, M. T., and Litt, T.: A method for climate and vegetation reconstruction through the inversion of a dynamic vegetation model, Clim. Dynam., 35, 371–389, 2010. 18482

Gaucherel, C., Campillo, F., Misson, L., Guiot, J., and Boreux, J.-J.: Parameterization of a process-based tree-growth model: comparison of optimization, MCMC and particle filtering algorithms, Environ. Modell. Softw., 23, 1280–1288, 2008. 18483, 18484

Geyer, C. J. and Johnson, L. T.: mcmc: Markov Chain Monte Carlo, available at: http://CRAN.R-project.org/package=mcmc, r package version 0.9-1, 2012. 18491
Goosse, H., Crespin, E., de Montety, A., Mann, M., Renssen, H., and Timmermann, A.: Reconstructing surface temperature changes over the past 600 years using climate model simulations with data assimilation, J. Geophys. Res., 115, D09108, doi:10.1029/2009JD012737, 2010. 18482
Guiot, J., Torre, F., Jolly, D., Peyron, O., Boreux, J.-J., and Cheddadi, R.: Inverse vegetation modeling by Monte Carlo sampling to reconstruct palaeoclimates under changed precipitation seasonality and CO_2 conditions: application to glacial climate in Mediterranean region, Ecol. Model., 127, 119–140, 2000. 18482
Guiot, J., Wu, H. B., Garreta, V., Hatté, C., and Magny, M.: A few prospective ideas on climate reconstruction: from a statistical single proxy approach towards a multi-proxy and dynamical approach, Clim. Past, 5, 571–583, doi:10.5194/cp-5-571-2009, 2009. 18482
Hastings, W. K.: Monte Carlo sampling methods using Markov chains and their applications, Biometrika, 57, 97–109, 1970. 18487
Hughes, M. and Ammann, C.: The future of the past – an earth system framework for high resolution paleoclimatology: editorial essay, Climatic Change, 94, 247–259, 2009. 18482
Keenan, T. F., Hollinger, D. Y., Bohrer, G., Dragoni, D., Munger, J. W., Schmid, H. P., and Richardson, A. D.: Increase in forest water-use efficiency as atmospheric carbon dioxide concentrations rise, Nature, 499, 324–327, 2013. 18496
LaMarche, V. C., Graybill, D. A., Fritts, H. C., and Rose, M. R.: Increasing atmospheric carbon dioxide: tree ring evidence for growth enhancement in natural vegetation, Science, 225, 1019–1021, 1984. 18481, 18496
Mann, M., Bradley, R., and Hughes, M.: Northern Hemisphere temperatures during the past millennium: inferences, uncertainties, and limitations, Geophys. Res. Lett., 26, 759–762, 1999. 18481
Mann, M. E.: The value of multiple proxies, Science, 297, 1481–1482, 2002. 18482
Mann, M. E., Zhang, Z., Hughes, M. K., Bradley, R. S., Miller, S. K., Rutherford, S., and Ni, F.: Proxy-based reconstructions of hemispheric and global surface temperature variations over the past two millennia, P. Natl. Acad. Sci. USA, 105, 13252–13257, 2008. 18481
McCarroll, D. and Loader, N. J.: Stable isotopes in tree rings, Quaternary Sci. Rev., 23, 771–801, 2004. 18482

BGD
10, 18479–18514, 2013

Invert modeling of tree rings

É. Boucher et al.

Title Page
Abstract | Introduction
Conclusions | References
Tables | Figures
◀| |▶
◀ ▶
Back | Close
Full Screen / Esc
Printer-friendly Version
Interactive Discussion

Medlyn, B., Badeck, F.-W., De Pury, D., Barton, C., Broadmeadow, M., Ceulemans, R., De Angelis, P., Forstreuter, M., Jach, M., Kellomäki, Š. S., Laitat, E., Marek, M., Philippot, S., Rey, A., Strassemeyer, J., Laitinen, K., Liozon, R., Portier, B., Roberntz, P., Wang, K., and Jarvis, P. G.: Effects of elevated [CO_2] on photosynthesis in European forest species: a meta-analysis of model parameters, Plant Cell Environ., 22, 1475–1495, 1999. 18496

Misson, L.: MAIDEN: a model for analyzing ecosystem processes in dendroecology, Can. J. Forest Res., 34, 874–887, 2004. 18483, 18484, 18492

Misson, L., Rathgeber, C., and Guiot, J.: Dendroecological analysis of climatic effects on Quercus petraea and Pinus halepensis radial growth using the process-based MAIDEN model, Can. J. Forest Res., 34, 888–898, 2004. 18483, 18484

Myhre, G., Highwood, E. J., Shine, K. P., and Stordal, F.: New estimates of radiative forcing due to well mixed greenhouse gases, Geophys. Res. Lett., 25, 2715–2718, 1998. 18481

Nicault, A., Guiot, J., Edouard, J., and Brewer, S.: Preserving long-term fluctuations in standardisation of tree-ring series by the adaptative regional growth curve (ARGC), Dendrochronologia, 28, 1–12, 2010. 18489

R Core Team: R: A Language and Environment for Statistical Computing, R Foundation for Statistical Computing, Vienna, Austria, available at: http://www.R-project.org/, ISBN 3-900051-07-0, 2012. 18491

Robertson, A., Overpeck, J., Rind, D., Mosley-Thompson, E., Zielinski, G., Lean, J., Koch, D., Penner, J., Tegen, I., and Healy, R.: Hypothesized climate forcing time series for the last 500 years, J. Geophys. Res.-Atmos., 106, 14783–14803, 2001. 18490

Schmidt, M., Graul, R., Sartorius, H., and Levin, I.: The Schauinsland CO_2 record: 30 years of continental observations and their implications for the variability of the European CO_2 budget, J. Geophys. Res.-Atmos., 108, 4619, doi:10.1029/2002JD003085, 2003. 18490

Schweingruber, F.: Tree Rings and Environment: Dendroecology, Paul Haupt, 1996. 18481

Sturm, K., Hoffmann, G., Langmann, B., and Stichler, W.: Simulation of $\delta^{18}O$ in precipitation by the regional circulation model REMOiso, Hydrol. Process., 19, 3425–3444, 2005. 18490

Tans, P. and Keeling, R.: Trends in carbon dioxide at Mauna Loa, available at: www.esrl.noaa.gov/gmd/ccgg/trends/, 2013. 18481

Tolwinski-Ward, S. E., Evans, M. N., Hughes, M. K., and Anchukaitis, K. J.: An efficient forward model of the climate controls on interannual variation in tree-ring width, Clim. Dynam., 36, 2419–2439, 2011. 18482

Vaganov, E. A., Hughes, M. K., and Shashkin, A. V.: Introduction and Factors Influencing the Seasonal Growth of Trees, Springer, 2006. 18481

BGD
10, 18479–18514, 2013

Table 1. Correlation between (1st column) observed and simulated climatic conditions in the Fontainebleau forest for the 1960–2000 period and (2nd column) correlation between tree rings and observed climatic conditions.

	Simulated vs. observed climate		Tree rings vs observed climate		
	T_{sim}	P_{sim}	TRW	$\delta^{13}C$	$\delta^{18}O$
T_{obs}	0.53	−0.3	−0.11	0.42	0.47
P_{obs}	−0.3	0.67	0.42	−0.51	−0.65

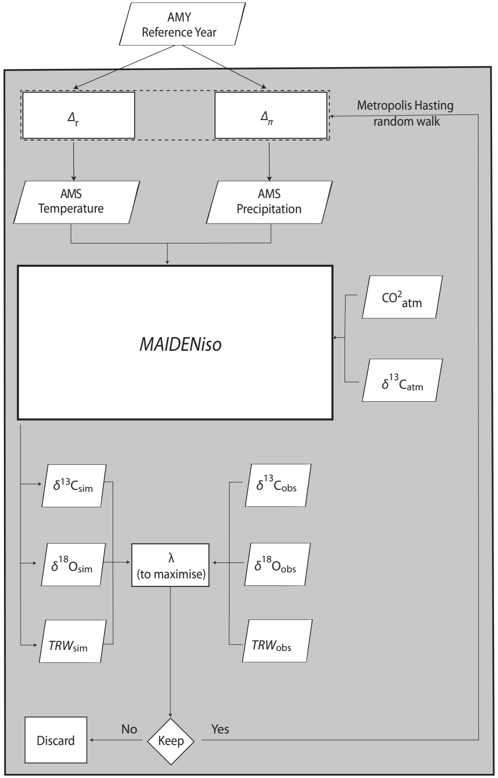

Fig. 1. MAIDENiso's inversion flowchart. For each year simulated, two Δ modify the AMY, one for temperature ($\Delta_{\tau t}$) and one for precipitation ($\Delta_{\pi t}$). The resulting AMS is passed to MAIDENiso, along with atmospheric CO_2 concentrations and atmospheric $\delta^{13}C$ to simulate tree growth parameters. Simulated tree growth is compared to observations, through the metric λ which has to be maximized (Eq. 1). The Metropolis Hastings iteratively modifies the value of Δ_τ and Δ_π so that it converges towards stable states (Eq. 2).

BGD
10, 18479–18514, 2013
Invert modeling of tree rings
É. Boucher et al.

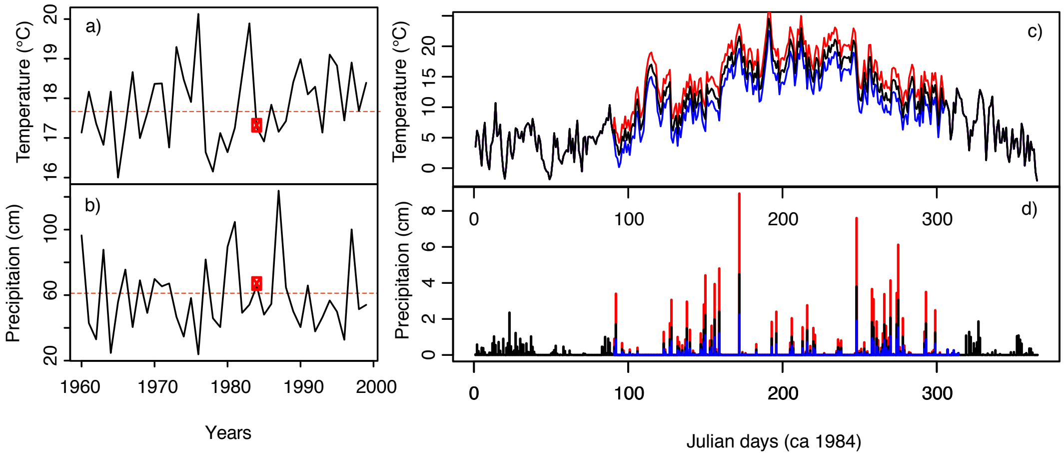

Fig. 2. Yearly and daily (1984) summer temperature and precipitation series for the Fontainebleau forest. The left panel presents temperature **(a)** and precipitation **(b)** series, with the AMY (1984) pointed as red squares. Average conditions are in dashed red. The right panel presents daily variations (in 1984) for temperature **(c)** and precipitation **(d)**. Black curves represent observations in 1984 (AMY). The red curves correspond to the AMS that results from the modification of the AMY by a Δ_τ of 2 and a Δ_π of 2. The blue curve represents an AMS that originates from the modification of the AMY by a Δ_τ of −2 and a Δ_π of 0.5.

BGD
10, 18479–18514, 2013

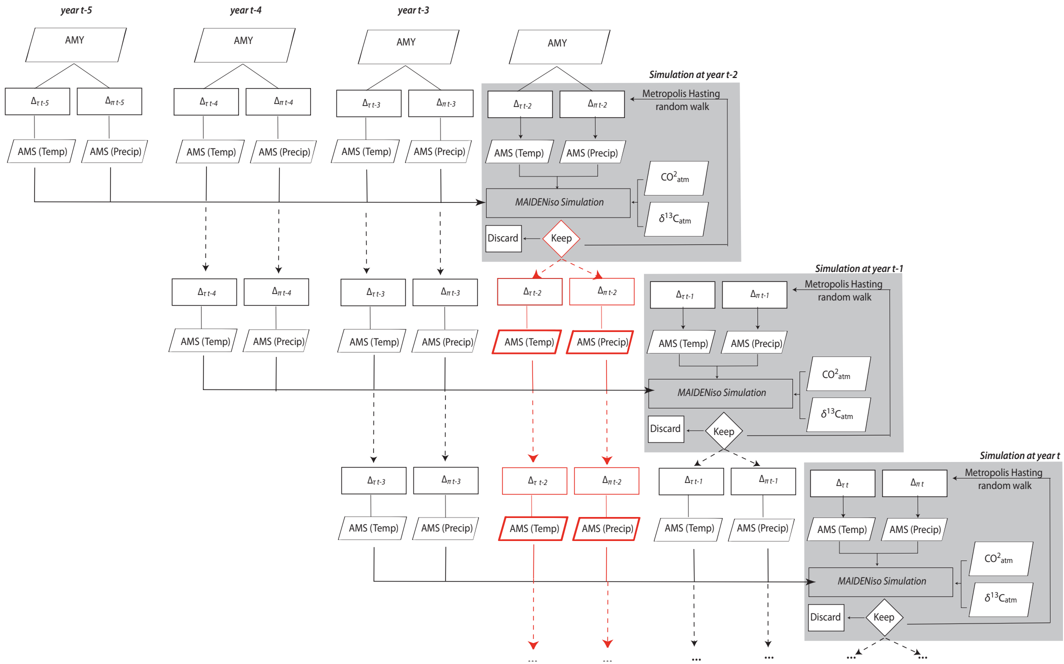

Fig. 3. Flowchart of the autocorrelation modeling. Each gray box corresponds to the inversion algorithm presented in Fig. 1. For each year t where the inversion is conducted, AMS from the three preceding years is also given as input to MAIDENiso, so the simulation is performed on a total of four years (bold arrows). Once the best combination of Δ is found by the Metropolis–Hastings, the mean δ values are passed to the next iteration. An example is given by red dashed lines. Δ found for year $t-2$ are also used to simulate $t-1$ and t.

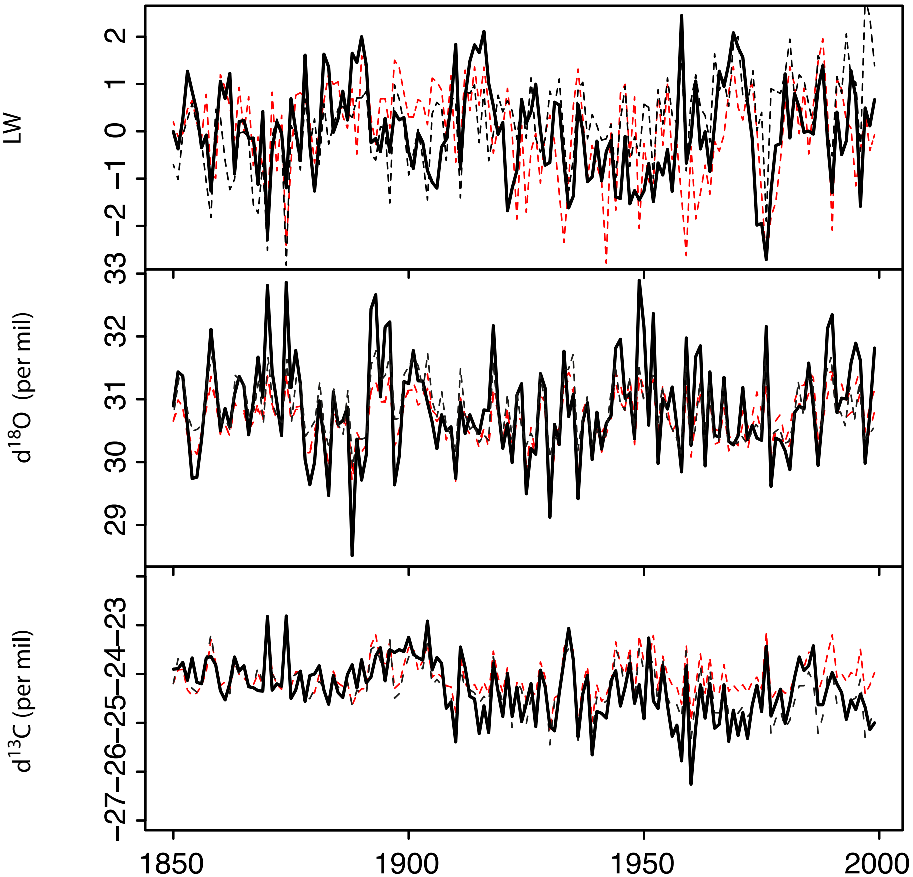

Fig. 4. Actual and simulated tree ring proxies. Black bold lines represent observed latewood widths (LW), $\delta^{18}O$ and $\delta^{13}C$ of tree ring α-cellulose. Black dotted lines correspond to the simulations performed from the A2 (increasing CO_2) scenario, while red dotted lines represent the A1 (stable CO_2) scenario.

BGD
10, 18479–18514, 2013

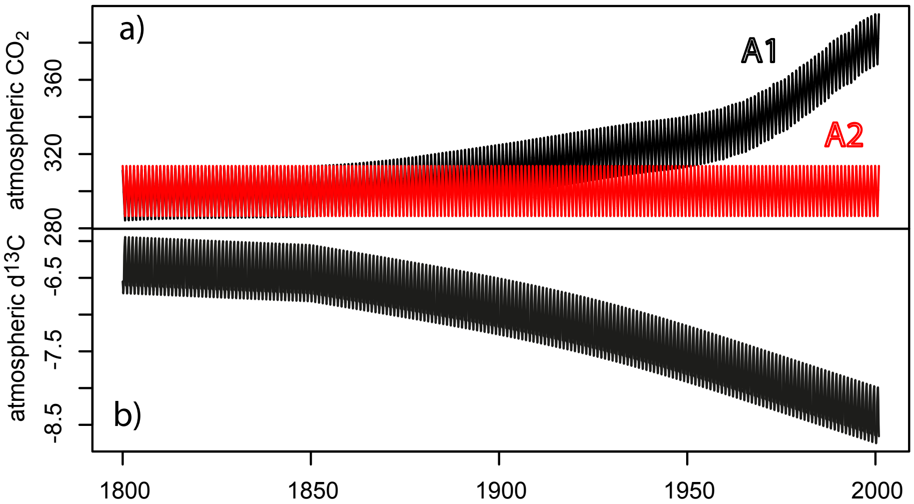

Fig. 5. Daily atmospheric CO_2 **(a)** and $\delta^{13}C$ **(b)** data used in the inversion. The A1 (black) scenario is a realistic one while scenario A2 (red) describes a hypothetical case where CO_2 concentrations would have remained at pre-industrial (1850) levels.

BGD
10, 18479–18514, 2013

Invert modeling of tree rings

É. Boucher et al.

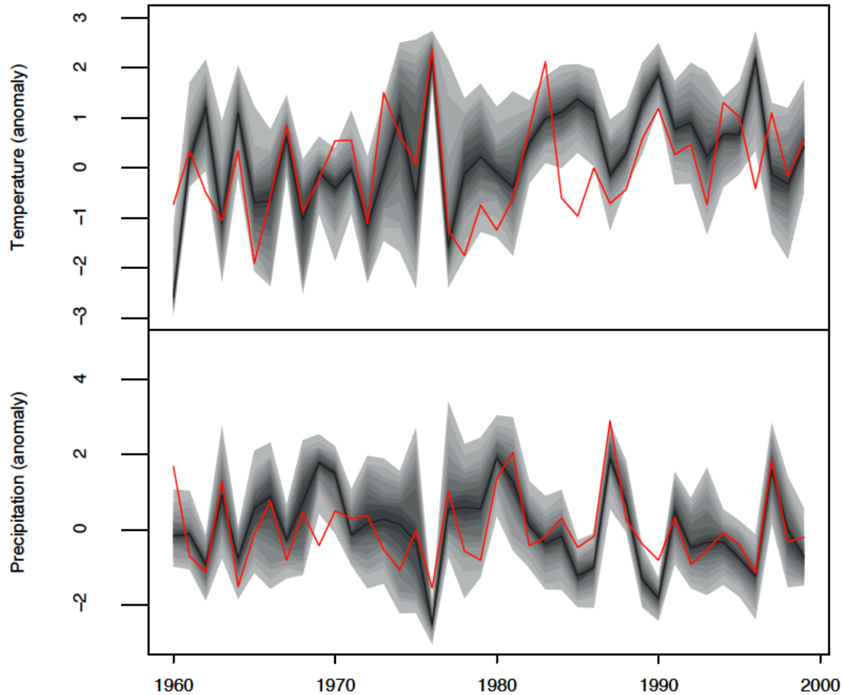

Fig. 6. Comparison with modern climatological records (1960–1999). Median reconstructed values correspond to the black curve, observations are in red. Quantiles 2.5 and 97.5 fall within the gray shading.

BGD
10, 18479–18514, 2013

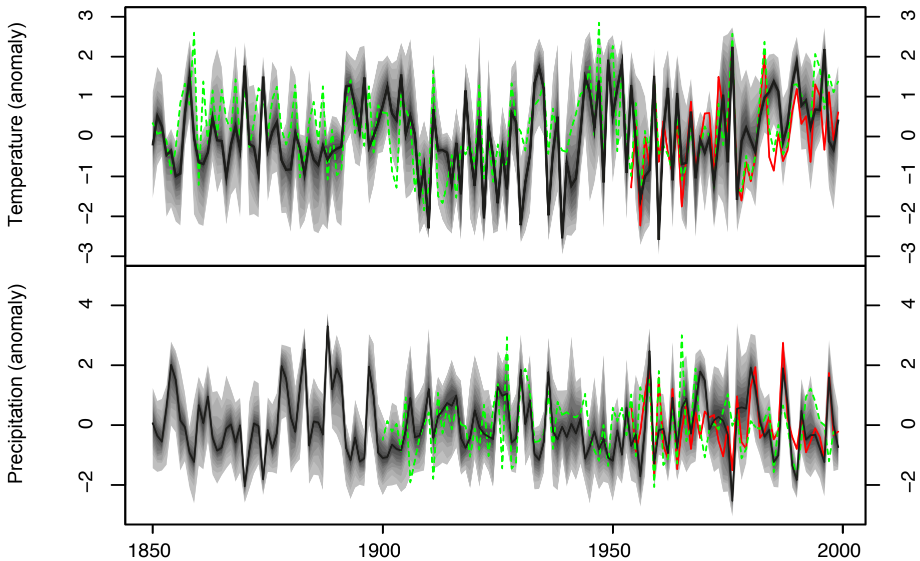

Fig. 7. Temperature and precipitation reconstructions back to ca 1850. Reconstructed climatic conditions (black) are compared to the CRU (green) data during the common period. Observations during the 1960–1999 period are in red. Quantiles 2.5 and 97.5 fall within the gray shading.

BGD
10, 18479–18514, 2013

Title Page
Abstract | Introduction
Conclusions | References
Tables | Figures
◂◂ | ▸▸
◂ | ▸
Back | Close
Full Screen / Esc
Printer-friendly Version
Interactive Discussion

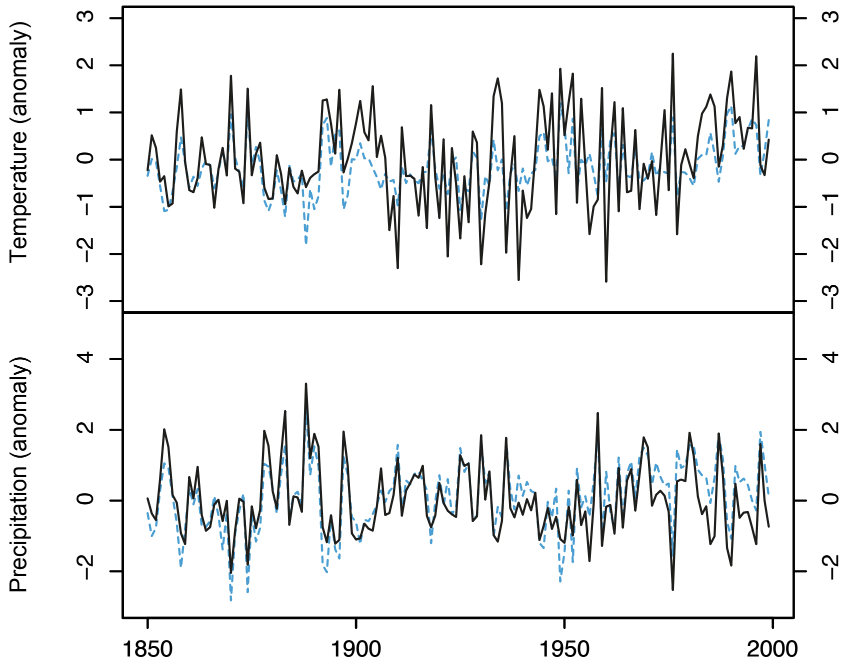

Fig. 8. Comparison between two reconstruction techniques: the inversion of MAIDENiso (black) and the transfer function (dashed blue) calibrated on the 1960–1999 period.

BGD
10, 18479–18514, 2013

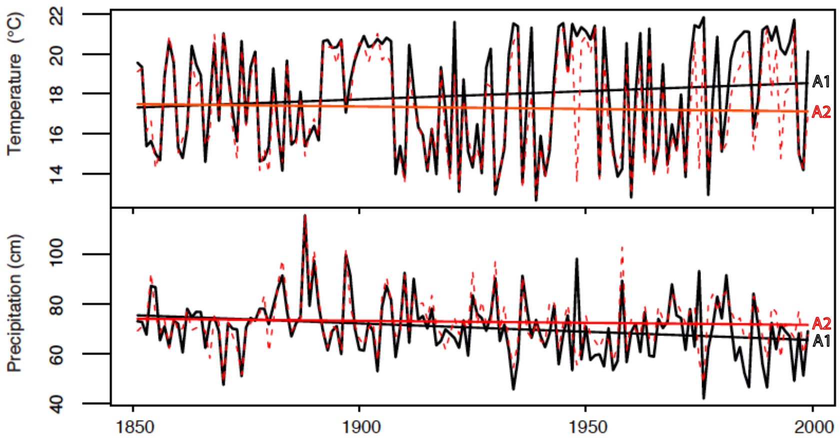

Fig. 9. Summer temperature and precipitation reconstructions driven by different CO_2 scenarios: A1 (black) and A2 (red).

BGD
10, 18479–18514, 2013

Invert modeling of tree rings

É. Boucher et al.

BGD
10, 18479–18514, 2013

Invert modeling of tree rings

É. Boucher et al.

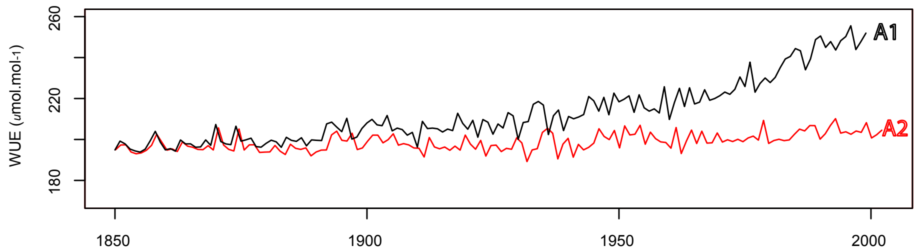

Fig. 10. Water use efficiency (WUE) changes for reconstructions performed using the A1 (black) and A2 (red) CO_2 scenarios.

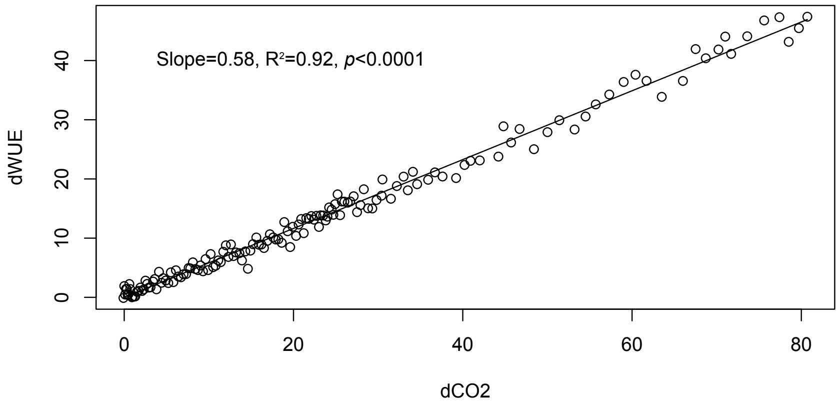

Fig. 11. Water use efficiency (WUE) changes with respect to changes in atmospheric CO_2. Both dCO_2 and dWUE were calculated from the difference between the A1 and the A2 scenario.

BGD
10, 18479–18514, 2013
Invert modeling of tree rings
É. Boucher et al.